

SPARSE POLYNOMIAL CHAOS-BASED SONIC BOOM UNCERTAINTY QUANTIFICATION AND AERODYNAMIC/SONIC BOOM ROBUST DESIGN OPTIMIZATION UNDER MULTI-PARAMETER UNCERTAINTIES

Shekun Wang¹, Huan Zhao², Keyao Gan³, Zhiyuan Gong⁴, Yvjie Gan⁵

¹⁻⁵School of Aeronautics, Northwestern Polytechnical University, Xi'an Shaanxi, 710072, China

Abstract

Uncertainty-considering aircraft sonic boom uncertainty quantification (UQ) and robust design optimization techniques have become one of the most promising ways to meet the design requirements of future environmentally friendly supersonic civil aircraft. However, traditional aerodynamic uncertainty quantification methods for aircraft are costly, narrowly applicable, and suffer from the curse of dimensionality. It is difficult to meet the demand for complex sonic boom multi-parameter UQ and aerodynamic/ sonic boom robust design optimization. To address this difficulty, first, this paper uses an efficient sparse polynomial chaos reconstruction method based on adaptive forward-backward selection (AFBS), combined with the augmented Burgers equation, to quantify the uncertainty of far-field sonic boom prediction. The AFBS method effectively enhances the sparsity of the PC reconstruction and improves the reliability of the fitting process. The augmented Burgers equation accurately simulates the far-field propagation of sonic boom. This part carries out sonic boom UQ considering six uncertain parameters: Mach number, altitude, temperature, humidity, wind direction, and wind velocity, and compares the results with the OMP method and the OLS method. The results indicate that the efficient sparse PC reconstruction method based on AFBS is less computational cost and accurate. It can be used for sonic boom UQ under multi-parameter uncertainties. Then an aerodynamic/sonic boom robust design optimization framework was constructed. Considering the uncertainty of Mach number and angle of attack, the lift, drag, moment coefficient, and PLdB were robustly optimized. The optimization results are improved in all metrics, proving that the optimization framework can be used for robust optimization of aerodynamic sonic booms.

Keywords: Sonic boom; Uncertainty quantification (UQ); Adaptive forward–backward selection (AFBS); Polynomial chaos expansion (PCE); Robust design optimization

1. Introduction

1.1 Low drag and sonic boom design

The trend towards globalization has led to closer economic and political ties between countries, as global transport networks become more sophisticated. This has contributed to the continued growth and prosperity of the civil aviation industry. With advances in science and technology and the targets of Carbon Peak and Carbon Neutrality, the next generation of aircraft aims to be comfortable, economical, safe, eco-friendly and high-speed. Faster flight speed remains an unchanging pursuit of mankind. However, the resulting sonic boom problem has become one of the core issues that limit supersonic civil aircraft development. To reduce the impact of sonic boom, researchers worldwide have conducted numerous studies. These studies have shown that the intensity of sonic boom can be influenced by various factors, including Mach number, altitude, atmospheric temperature and humidity. The interactions between these variables are complex, resulting in less robust sonic boom prediction and making it difficult to achieve the optimal sonic boom waveform. Traditional methods for sonic boom UQ are not only costly and narrowly applicable, but also face the curse of dimensionality. Therefore, these methods cannot meet the needs of sonic boom UQ.

In recent years, as the uncertainty problem in sonic boom prediction has become more and more apparent, this issue has received widespread attention and intensive study by many research institutions[1-4]. The current research mainly focuses on two main areas: the exploration of new optimization strategies, and in-depth studies on the selection of uncertainty parameters. Research in both directions is important to understand and improve the uncertainty in sonic boom prediction. Colonno et al.[5] review the currently accepted theories of sonic boom prediction and minimization and propose a new and improved method to overcome some of the limitations of the classical theory. However, the method is only a start for minimum sonic boom design under uncertainty. The paper also points out that good optimization strategies require not only high performance but also minimal sensitivity to uncertainty. This robust design approach is the subject of future study. Emre Tekaslan et al.[6] studied UQ using multifidelity methods for both sonic boom loudness and ground pressure signature while simultaneously considering flight and atmospheric parameters. By implementing multifidelity polynomial chaos expansion and multifidelity Monte Carlo methods, UQ tools were developed. However, its research has shown that MFMC is advantageous whenever the problem is high-dimensional, the correlation between the low- and high-fidelity simulation is high, and the cost of the low-fidelity simulations is notably cheaper. Inversely, MFPCE is propitious in case of a considerable low-fidelity simulation cost and a low-dimensional space. Thus, the method is less applicable. Makino et al.[7] investigated some metrics of sonic boom intensity used as an objective function for robust sonic boom minimization. This approach avoids sensitive low boom signatures obtained in sonic boom minimization using conventional sonic boom metrics. However, the disadvantage is that although the sonic boom metrics they presented have shown the importance of analytical robustness of the objective functions in sonic boom minimization, they do not necessarily guarantee that the sonic boom effects are minimized. Schaefer et al.[8] investigated the robust design of sonic boom using Spatially Accurate

Polynomial Chaos (SAPC) and applied the methodology to the design of a development version of the NASA X-59 QueSST aircraft. They found that the design based on SAPC increased robustness, but its drawback is the high computational cost. Rallabhandi et al.[9] developed a method to solve propagation uncertainty during the minimization of sonic boom using a discrete adjoint method. It takes into account the uncertainty in atmospheric inputs. The advantage of this method is that it minimizes both the mean and standard deviation and it is less computational cost. But the limitation of this method is that it only considers the uncertainty in the atmospheric parameters. The above methods have made some progress in the field of sonic boom uncertainty, but all have some limitations.

1.2 Robust design optimization

In the field of aerodynamic design optimization, the traditional deterministic-based design optimization method only considers the aerodynamic performance parameters at the design point and does not consider the drastic changes in aerodynamic performance that may be caused by various sources of uncertainty. Therefore, the results obtained by this kind of design optimization have poor robustness. It is often difficult to maintain stable aerodynamic performance when affected by uncertain factors, and even causes a sharp deterioration in performance. Therefore, the results of single-point deterministic design are difficult to be applied in engineering. Multi-point deterministic design attempts to obtain usable results by constraining several state points, but it will face difficulties in implementation as the number of uncertain factors considered increases. The uncertainty-based design optimization method considers the impact of uncertain sources on performance during the optimization process and looks for designs that are insensitive or do not fail when the uncertain sources change. It is a more valuable design method than deterministic design.

NASA Langley Research Centre in its white paper [10] states that it is very important to consider the effects of various possible uncertainties. And with the development of computational power and various advanced uncertainty analysis and design methods, uncertainty-based design can make the design results more robust. In recent years, with the development of the world's aviation industry, economic, green, and safe flying vehicles are getting more and more attention. Aerodynamic shape design considering uncertainty can provide more robust aerodynamic performance in the face of complex flight conditions, which meets the current performance requirements of aircraft.

Uncertainty-based design problems fall into two categories: robust design problems and reliability-based design problems [10]. A robust design problem seeks a design that is relatively insensitive to small changes in uncertain inputs. The reliability-based design problem seeks a design whose probability of failure is less than some acceptable value. The same mathematical formulas can be used to describe both robust and reliability-based design, however their areas of application are quite different. The design domains in which they are applied are illustrated in Figure 1: for extreme events that could result in catastrophe, we would prefer to use reliability-based optimal design. Whereas for routine events with lesser impact, it is more expected to make the performance insensitive to normal fluctuations, i.e. robust design optimal. The two are also concerned with different regions of distribution of the probability density function. Robust design is concerned with the probability distribution near the

mean of the probability density function, while reliability-based design is concerned with the probability distribution at both ends of the probability density function, as shown in Figure 2. Among them is the uncertainty-based aerodynamically robust optimal design method for aircraft that considers the effect of uncertainty on aerodynamic performance during the optimization process. The design with less sensitivity to uncertainty factors is searched for to obtain robust design results.

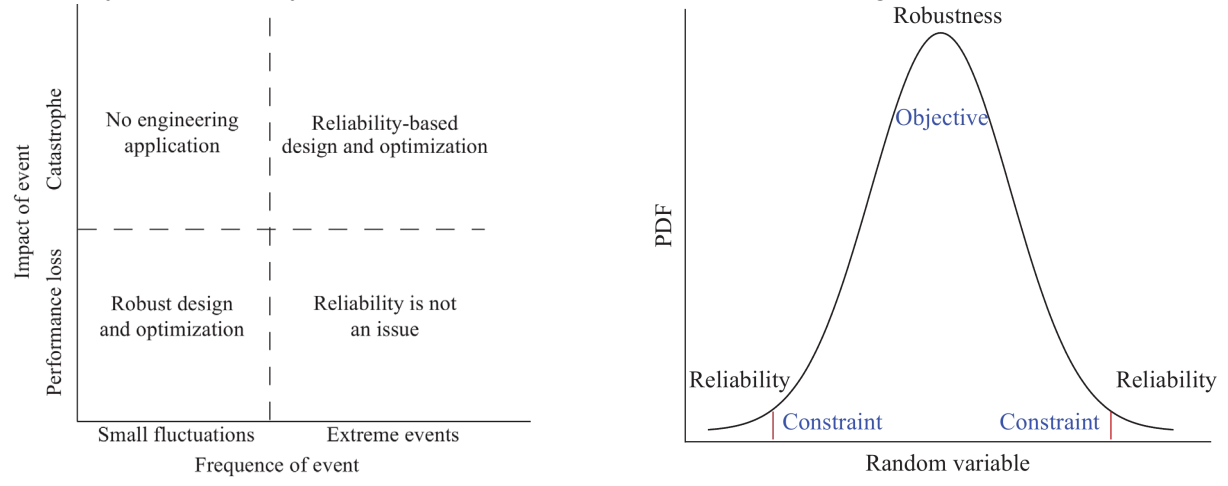


Figure 1 – Uncertainty-based design domains

Figure 2 – Probability Density Function Distributions for Reliability and Robustness Design Concerns

There are many methods available for the aerodynamic uncertainty analysis and robust design of aircraft. Aerodynamically robust design optimal can provide robust and reliable aerodynamic configurations under possible uncertainties in the flight envelope and throughout the life cycle of the vehicle and reduce costs. The main problems faced today are how to address the high computational cost, the increasing dimensionality of uncertainty, and the complexity of the aerodynamically robust optimal design procedure. These hinder the wider application of Aerodynamic Robust Design Optimization (RADO).

Zhao [11] et al. introduced the non-uniform free-form deformation (NFFD) method based on non-uniform rational B-spline (NURBS) basis functions into airfoil parameterization. The non-dominated sorting genetic algorithm-II (NSGA-II) was used as the search algorithm. An agent model based on the Kriging model is introduced to improve the efficiency of the optimization system. A transonic, high Reynolds number natural laminar flow airfoil is designed and investigated to achieve robust design with Mach number uncertainty. Zhao [12] and others developed an Uncertainty-Based Design Optimization (UBDO) framework based on the polynomial chaos expansion method. A particle swarm optimization algorithm combined with an agent model was used to search for optimal natural laminar flow airfoils. By weighing aerodynamic performance under fully turbulent and free turning conditions. The optimal airfoil shape is obtained by maintaining robust and reliable aerodynamic performance under complex flight conditions. Huang [13] et al. investigated the aerodynamically optimized robust design of supercritical airfoils considering fuselage disturbances. The aerodynamic robust design optimization system consists of a genetic optimization algorithm, an improved Back Propagation (BP) neural network

and a deformation grid technique. Two major improvements are made to the BP neural network to increase the training speed and accuracy. The optimized wing not only has better aerodynamic characteristics, but the intensity of the excitation wave is also reduced.

Zhao [14] et al. developed a sparse polynomial chaotic reconstruction method based on Adaptive Forward-Backward Selection (AFBS), which greatly improved the uncertainty analysis and robust optimization efficiency. An efficient aerodynamic robust design optimization method considering multiparameter uncertainties is also developed. The method effectively solves the difficulty of the traditional airfoil design method to meet the high speed and high lift natural laminar flow airfoil design requirement of taking into account the high lift design, natural laminar flow design, and supercritical design.

Keane [15] used Cokriging for optimization of gas turbine compressor blades using a multi-objective optimization scheme that takes into account uncertainties in manufacture, operating conditions, and degradation in operation. Pseudo-Monte Carlo sampling was used to propagate uncertainties during the analysis and combined with a state-of-the-art multi-fidelity approach to limit the runtime of the optimization process. The results show that an explicit balance between performance and robustness is achieved, guaranteeing good performance with small variations in performance. Hosder [16] et al. proposed an inexpensive Non-Intrusive Polynomial Chaos (NIPC) method for propagating input uncertainty in CFD simulations. Since the method is non-intrusive and does not require modification of the deterministic code, the method can be used directly for any stochastic fluid dynamics problem and its computational cost is lower than non-intrusive methods based on sampling or quadrature. Shah [17] et al. have developed a method to propagate the input uncertainties in CFD simulations by using the Quantification of Margins and Uncertainties (QMU) approach to implement Dempster-Shafer evidence theory for reliability and performance assessment of complex engineering systems in the presence of mixed uncertainties (chance and multiple sources of knowledge). Padron [18] et al. introduced a multifidelity approach to achieve high-fidelity robust optimization. Their multi-fidelity approach uses a polynomial chaotic expansion constructed from a combination of low-fidelity models and model corrections to approximate the high-fidelity statistics and statistical gradients used in each optimization iteration. The results show computational savings of 60% to 90% when compared to high-fidelity optimization. Dodson [19] et al. investigated the potential of the polynomial chaotic approach used in conjunction with computational fluid dynamics to quantify the computational effects of uncertainty in the aerodynamic design process. A polynomial chaos theory and a non-intrusive spectral projection implementation were proposed and used to demonstrate polynomial chaos as a basis for robust optimization, focusing on how to maximize the lift-to-drag ratio of a two-dimensional airfoil while minimizing its sensitivity to leading edge thickness uncertainty. The results show that the global optimum of certain design problems cannot be reached without taking uncertainty into account.

1.3 Current challenges

Aerodynamic design optimization methods should first of all be applied techniques to meet complex engineering requirements. The complexity of the flow field characteristics, such as viscous, compressible, separated flow, turning, surge and other nonlinear flow characteristics, is very sensitive

to the uncertainty of the flight state (e.g., Mach number, angle of attack, turbulence, etc.) and the shape change (deformation, machining error, etc.), which makes the shape designed by the traditional deterministic design method drastically change the aerodynamic performance in the face of the uncertainty factors. Aerodynamically robust design is a very effective advanced design technique to solve the above problems, but the current aerodynamically robust design method suffers from the complexity of the application process and the huge computational cost. At each step of the robust optimization process, uncertainty quantification and analysis is performed for each candidate aerodynamic shape, which significantly increases the computational cost of uncertainty quantification compared to a single CFD analysis, and thus the time for robust optimization increases significantly compared to deterministic optimization. Traditional uncertainty analysis techniques such as Monte Carlo Simulation (MCS) are costly and very inefficient for robust design optimization. Moreover, as more and different types of uncertainties need to be considered for complex aerodynamic shape optimization problems, the efficiency of robust optimization decreases further, and the problem of huge computational cost is encountered. Robust optimization also increases the number of objectives exponentially, especially for multi-objective robust optimization problems, which deepens the problem of high-dimensional multi-objective optimization. Currently applicable to the development of robust optimization techniques for aerodynamic design problems is still very slow, especially the aerodynamic uncertainty analysis is still encountered in the high computational cost of the problem, making it difficult to get a wide range of engineering applications.

Robust optimization of sonic boom will face the optimization strategy and uncertainty parameter selection and other issues. A good optimization strategy not only needs to be high performance, but also need to minimize the sensitivity to uncertainty. The selection of uncertainty parameters will help to optimize the sonic boom to obtain an insensitive low sonic boom characteristics, so as to obtain a robust design of low sonic boom.

The above challenges hinder the development of robust design optimized for aerodynamic/sonic boom.

1.4 Research in this paper

Aiming at the above problems, this paper introduces the basic theory, main methods and key technologies of aerodynamic robust design optimization methods. Especially for the problem that traditional uncertainty analysis methods have a narrow scope of application or are costly, an efficient sparse PCE reconstruction method and an efficient uncertainty analysis method based on sparse PCE are used, and an efficient sonic boom uncertainty quantification and aerodynamic/sonic boom robust design optimization method considering multi-parameter uncertainty are established to meet the design requirements of complex engineering problems.

2. Theory of sparse PCE

2.1 Polynomial chaos expansion

Among uncertainty analysis methods, Polynomial Chaos Expansion (PCE) is a powerful meta-modeling tool as an efficient theory of probabilistic uncertainty propagation and quantification. It has important applications in many engineering and applied mathematics fields, including structural reliability, sensitivity analysis, Monte Carlo simulation, etc. Among them, Wiener-Askey PCE and generalized polynomial chaos expansion (GPCE) are used as adaptable stochastic agent models. The correspondence between univariate autocovariate types and corresponding orthogonal polynomial types in Wiener-Askey PCE satisfies the Askey scheme [20] and has been widely used in uncertainty quantification.

Consider a probability space (Ω, Θ, P) , where Ω is a sample space, Θ is an appropriate σ -algebra on Ω , and P is a probability measure on (Ω, Θ) . Assume real-valued random variables and stochastic processes $f \in L^2(\Omega)$ defined in a probability space (Ω, Θ, P) that are expressed as:

$$f(\Xi) = a_0 \Gamma_0 + \sum_{i_1=1}^{\infty} a_{i_1} \Gamma_1(\xi_{i_1}) + \sum_{i_1=1}^{\infty} \sum_{i_2=1}^{i_1} a_{i_1,i_2} \Gamma_2(\xi_{i_1}, \xi_{i_2}) + \sum_{i_1=1}^{\infty} \sum_{i_2=1}^{i_2} a_{i_1,i_2,i_3} \Gamma_3(\xi_{i_1}, \xi_{i_2}, \xi_{i_3}) + \cdots$$
 (1)

Where: Γ_k represents a polynomial of order k; coefficient a is a real number; and $\Xi = (\xi_1, \xi_2, \dots \xi_d)$ represents a collection of mutually independent random variable inputs. Further, the above formula can be simplified as:

$$f(\Xi) = \sum_{i=1}^{\infty} \alpha_i \psi_i(\Xi)$$
 (2)

Where, α_k and ψ_k in (2) correspond to a and Γ_k in (1). Eq. (2) is truncated at order p and can be expressed as:

$$f(\Xi) = \sum_{|k| \le p} \alpha_k \psi_k(\Xi) = \sum_{i=1}^{M_p} \alpha_i \psi_i(\Xi) + \varepsilon(\Xi)$$
(3)

Where: M_p represents the number of polynomial terms remaining after truncation; α_i is the coefficient of the k-th basis function of PCE, and ψ_i is the k-th basis function; $\varepsilon(\Xi)$ is the truncation error, and the truncation strategy is the key factor affecting the truncation error; α_i is the coefficient of the i-th basis function of PCE; and ψ_i is the i-th basis function. Due to the orthogonality of the PCE basis functions, their statistical properties can be easily obtained by calculation, and the expressions for the mean value μ_f and standard deviation σ_f are as follows:

$$\mu_f = \mathcal{E}(f(\Xi)) = \alpha_1 \tag{4}$$

$$\sigma_f^2 = \mathbf{E}(f(\Xi) - \mathbf{E}(f(\Xi)))^2 = \sum_{i=2}^{M_p} \alpha_i^2 \left\langle \psi_i^2 \right\rangle$$
 (5)

Therefore, the first- and second-order moments of the response function can be quickly estimated by simply requiring the polynomial expansion coefficients, i.e., the PCE reconstruction.

PCE reconstruction is the process of recovering polynomial coefficients based on input variables and output responses. Popular methods include the Galerkin projection (GPNIPC) and the point collocation

method (also called least squares). The GPNIPC derives the coefficients of each basis function by projecting the output response in the direction of each basis vector, where due to orthogonality, just the same basis projection/inner product is not equal to zero. It exacts the maps between uncertainties inputs and performance, and gets PC coefficients by:

$$\beta_{i} = \frac{\left\langle f(\Xi), \psi_{i} \right\rangle}{\left\langle \psi_{i}^{2} \right\rangle} = \frac{\int f(\Xi)\psi_{i}(\Xi)\xi(\Xi)d\Xi}{\left\langle \psi_{i}^{2} \right\rangle}, \quad i = 1, 2, \dots, M$$
(6)

where the computational cost of this strategy is typically dominated by the computation of the projection integration $\langle f(\Xi), \psi_i \rangle$ for every β_i . Popular approaches to computing $\langle f(\Xi), \psi_i \rangle$ include Monte Carlo (MC) evaluation and numerical integral formula. MC evaluation in Eq.(7), where N denotes the number of observed samples points.

$$\langle f(\Xi), \psi_i \rangle = \frac{1}{N} \sum_{j=1}^{N} f(\Xi^{(j)}) \cdot \psi_i(\Xi^{(j)})$$
 (7)

The numerical integral formula computes the integration by Eq.(8).

$$\langle f(\Xi), \psi_i \rangle = \sum_{i_1}^{N_1} \cdots \sum_{i_n}^{N_n} A_{i_1} \cdots A_{i_n} f(\zeta_{i_1}, \zeta_{i_2}, \dots, \zeta_{i_n}) \psi_i(\zeta_{i_1}, \zeta_{i_2}, \dots, \zeta_{i_n})$$
 (8)

where N_j indicates the number of integration point of the j-th dimensionality, A_i and $(\zeta_{i_1},\zeta_{i_2},...,\zeta_{i_n})$ denote the i-th weight and node, respectively.

As the dimension d increases, the number of integration points will increase exponentially and the GPNIPC faces the challenge of huge computational cost.

The point collocation method can fit the basis function coefficients using least squares regression, which is given by

$$\beta = (\Psi^T \Psi)^{-1} \Psi^T Y \tag{9}$$

 $\beta = (\Psi^T \Psi)^{-1} \Psi^T Y \tag{9}$ where $\Psi = \left\{ \psi_i(\Xi^{(j)}) \right\}$ is the measurement matrix containing samples of the PC basis, and $Y = (f(\Xi^{(1)}), f(\Xi^{(2)}), \ldots, f(\Xi^{(N)}))^T$ contains the response of the observed points. $\beta = (\beta_1, \beta_2, ..., \beta_M)^T$ denotes the vector of PC coefficients.

However, the number of PCE truncation terms increases geometrically with the number of spatial dimensions and the order of unfolding, which leads to a sharp increase in the number of samples required to fit the truncated PCE terms, and the approximation accuracy is difficult to be guaranteed, i.e., the problem of dimensional catastrophe. For the aerodynamic problem, the high confidence computational samples are usually considered to require large computational costs and are usually confronted with high-dimensional higher-order responses to the effects of complex three-dimensional shapes and compressibility. The dimensional catastrophe problem will be a great obstacle to limit the application of PCNIPC (point collocation nonintrusive polynomial chaos) method to high-dimensional complex problems. To address this difficulty, the matching point method based on the theory of compressed sensing [21] can effectively alleviate the dimensional catastrophe problem by identifying and recovering the most important PC terms and their coefficients, and constructing sparse PCE theories and methods [22]. Some popular sparse PCE methods include least angle regression (LAR)

[23], orthogonal matching pursuit (OMP) [24], adaptive forward-backward selection (AFBS) [14], weight ℓ_1 -minimization [25], gradient enhancement ℓ_1 -minimization [26], multifidelity ℓ_1 - minimization [27] and other algorithms have been widely used and obtained very good performance in many complex problems.

2.2 Sparse polynomial chaos representation

For a large number of expansions of polynomial chaos, not all of the terms make a significant contribution to the output response, and many of the terms make a small or even zero contribution. Therefore, if these large contributors can be effectively identified and only the coefficients of these significant contributors can be recovered, the computational cost will be greatly reduced. Therefore, combining this effective idea with the compression-aware theories and methods that have been widely used in the field of information data recovery in recent years, some researchers have proposed a number of effective ways to solve the problem, which are collectively referred to as sparse PCE reconstruction methods.

Compressed sensing is used for sparse polynomial chaos reconstruction, where an efficient algorithm to find the minimum number of polynomial terms with non-zero coefficients, constructing exact PC representations with a small number of collocation points excites the search for a sparse approximation β . The ℓ_0 -minimization directly provides an optimally sparse approximation $\mathbf{C} = \{\beta_i \mid \beta_i \neq 0\}$, with the minimum number of non-zero entries, and restores β back to within ε in the L_2 , namely

$$\min_{\beta} \|\beta\|_{0}, \quad s.t. \|\psi\beta - \mathbf{Y}\|_{2} \le \varepsilon \tag{10}$$

The above equation is the ℓ_0 -minimization problem. where $\mathbb{C} = \{\beta_i \mid \beta_i \neq 0\} = \|\beta\|_0$ represents the number of non-zero polynomial terms and \mathcal{E} represents the approximation error. Obviously, the ℓ_0 -minimization problem is an NP-hard problem, i.e., solving Eq.(10) directly will result in a huge computational expense. Therefore, some studies have pointed out that by relaxing the ℓ_0 -minimization problem into an ℓ_1 -optimization problem

$$\min_{\beta} \|\beta\|_{1}, \quad s.t. \|\psi\beta - \mathbf{Y}\|_{2} \le \varepsilon \tag{11}$$

The ℓ_1 -optimization problem represented by Eq.(11) is also known as the BPDN (basis pursuit denoising) problem, where $\|\beta\|_1 = |\beta_1| + |\beta_2| + \cdots$. However, the ℓ_0 -optimization problem (Eq.(10)) and the ℓ_1 -optimization problem (Eq.(11)) are not completely equivalent unless a specific condition is satisfied: ℓ_0 -optimization and ℓ_1 -optimization are equivalent when the measurement matrix Ψ satisfies the RIP (Restricted Isometry Property) property.

The ℓ_1 -minimization problem represented by Eq.(11) can be solved by a large number of efficient algorithms. These algorithms include basis pursuit and greedy algorithms, OMP and LAR are widely used greedy algorithms.

Least angle regression (LAR), also including Stagewise algorithms and Lasso algorithms [23], can be regarded as the conservative forward greedy algorithm or less greedy version of the traditional forward selection methods. LAR has less greediness and is a classical LASSO algorithm. Due to these excellent properties, Blatman and Surdret [28] used least-angle regression for reconstructing sparse PCE, and it

AERODYNAMIC/SONIC BOOM ROBUST DESIGN OPTIMIZATION

has been widely used. The process of minimum angle regression for sparse PCE reconstruction is as follows: LARs start with all coefficients given zero values and find the predictor most correlated with the response to be added to the active set. The first prediction step is considered in the direction of this predictor until other predictor has as much correlation with current residual. The predictor will be added to the active set. Next, LARs adjust the coefficients in a direction equiangular between these predictors of active set, until some other predictor has as much correlation with the current residual. In the iteration procedure, the new predictor is added to the active set and performing forward selection again until the stopping criterion is reached.

3. AFBS applied to sonic boom uncertainty quantification

3.1 Experimental design

In this chapter, the supersonic concept airliner Lockheed Martin 1021 (LM1021) provided by the Second Sonic Boom Prediction Workshop (SBPW2) is used as a standard model. The azimuth angle is taken as 0° and the near-field overpressure distribution is shown in Figure 3. The propagation of the sonic boom is simulated by the code in [29], which solves the augmented Burgers equation considering the atmospheric attenuation. It is verified that the code can accurately simulate the propagation process of sonic boom. In analyzing the propagation of sonic boom to the far field, there are six uncertain parameters considered in this paper, which are: temperature T, humidity h, wind speed V, wind direction ϕ , flight altitude H, and Mach number Ma. Assume the six parameters are normally distributed. The variation of temperature with height was taken from computing formula[30]. The variation of wind speed, wind direction, and humidity with height were taken from real data for a region in December. These data were taken as fixed values μ_i of the parameters and made into uncertain variables by adding a normally distributed uncertainty term ξ_i after them of the form: $\mu_i + \xi_i \dots (i = T, h, V, \phi)$, where: $\xi_T \sim N(0, 2)$, $\xi_h \sim N(0, 8)$, $\xi_V \sim N(0, 2)$, $\xi_\phi \sim N(0, 10)$. The Mach number distribution satisfies $Ma \sim N(1.6, 0.03)$ and the flight altitude distribution satisfies $H \sim N(16764,100)$. The following section analyses the uncertainty of sonic boom propagation in the atmosphere using AFBS and compares it with other methods.

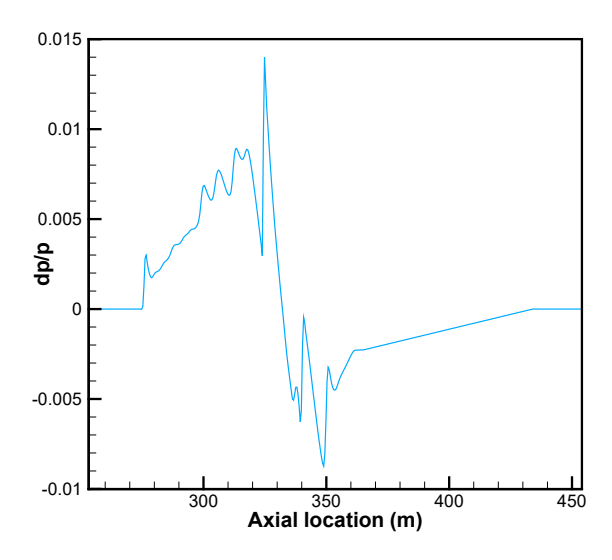


Figure 3 – Near-field overpressure distribution of LM1021

3.2 Comparison of AFBS, OMP and MCS methods for predicting ground sonic boom signature.

The mean of ΔP estimated by the AFBS, OMP, and MCS methods are shown in Figure 4. The relative errors of the mean of ΔP for AFBS with different samples (N = 30, 50, 100) are shown in Figure 5. The results indicate that the mean obtained by the AFBS method with 30 samples is almost the same as that obtained by the MCS method with 20,000 samples. The relative error of the mean decreases as the AFBS sample increases. The standard deviations of ΔP estimated by the AFBS, OMP, and MCS

methods are shown in Figure 6. The relative errors of the standard deviations of ΔP for AFBS with different samples (N = 30, 50, 100) are shown in Figure 7. The results indicate that the standard deviation obtained by the AFBS method with 30 samples is close to the standard deviation of the MCS method with 20,000 samples. The relative error of the standard deviation decreases as the AFBS sample increases. Note that only times between 0.13 and 0.47 seconds are considered in the calculation of the relative error, because in the rest of the range, ΔP is almost zero, so the results are strongly influenced by numerical noise. A comparison of the exact value of the ground signature with the $\pm 2\sigma$ range of ΔP estimated by AFBS with 30 samples is given in Figure 8. The relative errors of ΔP predicted by AFBS with different samples are given in Figure 9. It can be found that as the samples increases, the relative error of ΔP gradually decreases and the curve becomes progressively smoother. These results indicate that the AFBS method is efficient for reconstructing sparse PC representation and can be applied to estimate ground sonic boom signature at arbitrary accuracy levels. The AFBS method produces a sparser and more accurate PC metamodel than the other two methods. It is worth noting that the AFBS method requires fewer samples to achieve the same level of accuracy as the OMP and OLS methods.

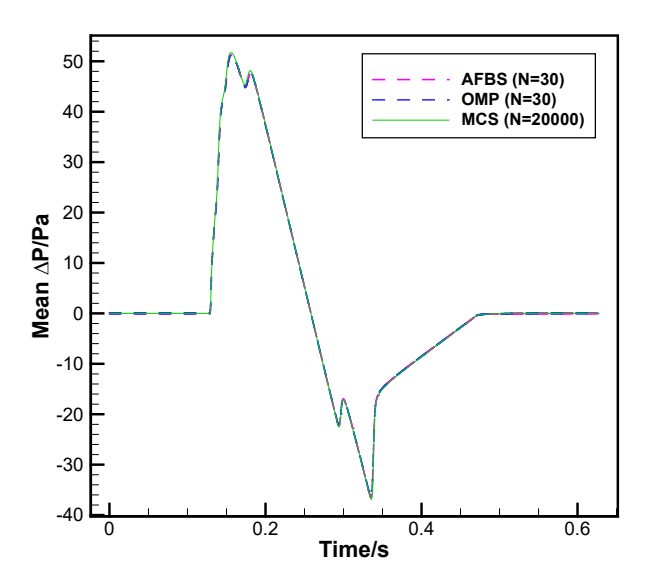


Figure 4 – Comparison of mean of ground signatures estimated by AFBS, OMP, and MCS.

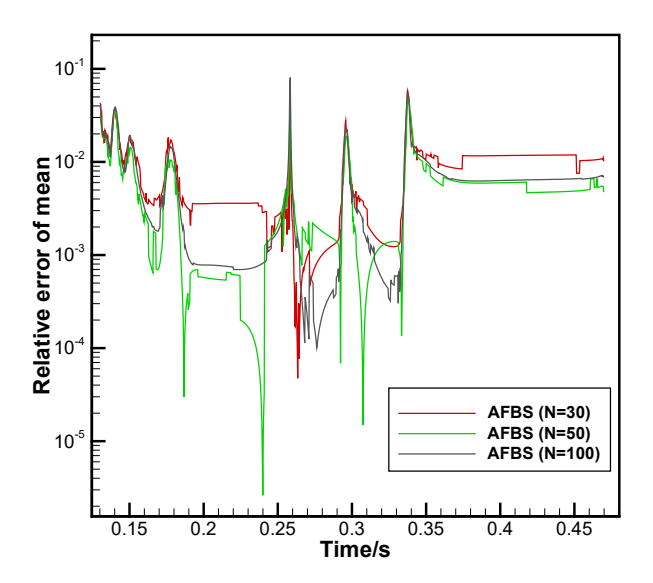


Figure 5 – Relative error of mean of ground signatures estimated by AFBS with different samples (0.13 s \leq t \leq 0.47 s).

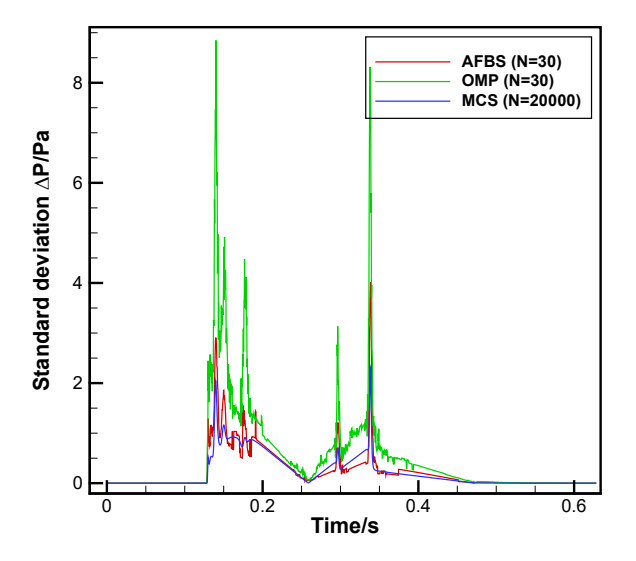


Figure 6 – Comparison of standard deviation of ground signatures estimated by AFBS, OMP, and MCS.

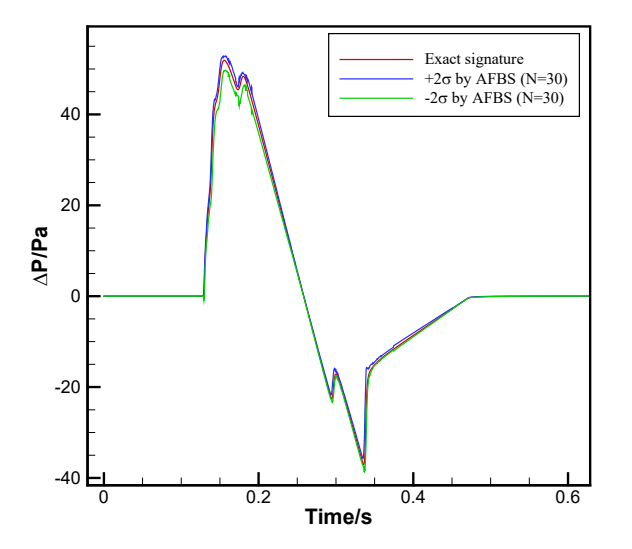


Figure 8 – The $\pm 2\sigma$ range of the ground signature estimated by AFBS with 30 samples.

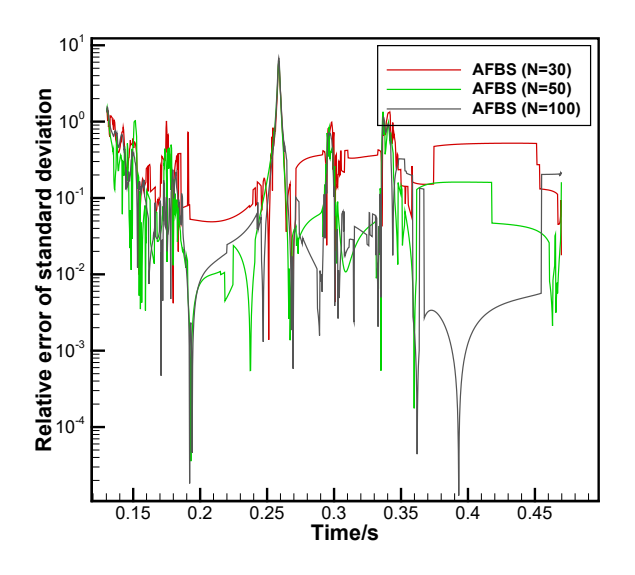


Figure 7 – Relative error of standard deviation of ground signatures estimated by AFBS with different samples (0.13 s \leq t \leq 0.47 s).

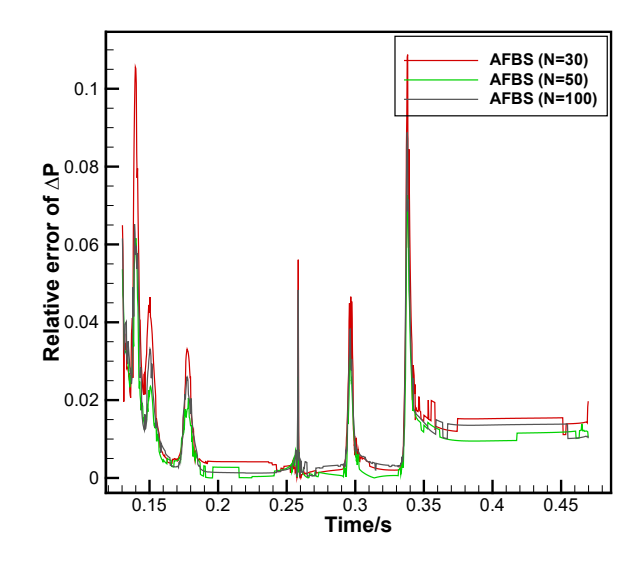
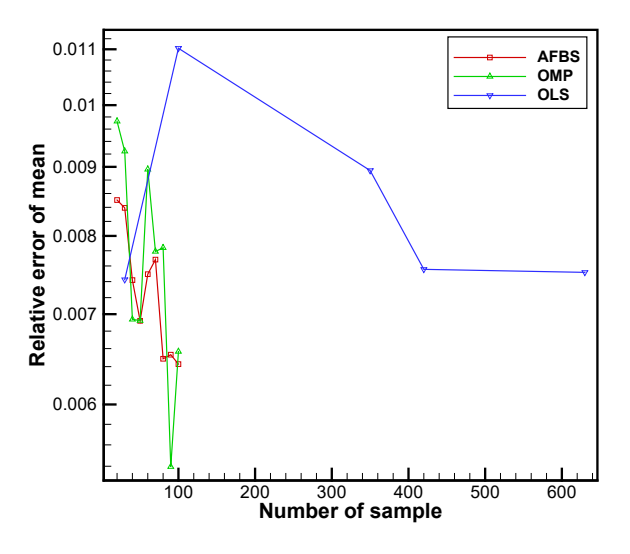


Figure 9 – Relative error of ΔP predicted by AFBS with different samples.

3.3 Convergence of AFBS, OMP and OLS methods with sample size

Figure 10 and Figure 11 show the convergence of the relative errors of the mean and standard deviation of ΔP obtained by the AFBS, OMP, and OLS methods at one point with samples increasing. The sample point is taken in the region of the peak of the ground waveform in order to make the results significant. The results indicate that as the samples increases, OLS converges the slowest, OMP follows, AFBS is the fastest, and AFBS has best stability after convergence. The AFBS method achieves small relative errors and the fastest convergence speed than the other two methods. The results again indicate that the AFBS method requires the minimum number of samples with a high level of accuracy compared to the OMP and OLS methods.



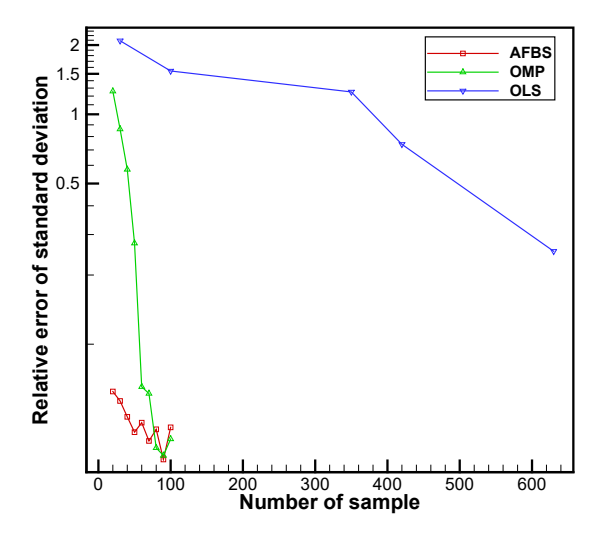


Figure 10 – Comparison of relative errors of mean of AFBS, OMP, and OLS method.

Figure 11 – Comparison of relative error of standard deviation of AFBS, OMP, and OLS method.

3.4 Robustness of AFBS, OMP and OLS methods to sample

UQ requires a certain number of samples to be taken, and different samples obtained different results. while the samples are randomly taken. It is necessary to ensure the robustness of the results while the samples are different. In the following, the results are calculated 100 times for each of the three methods with different samples. The robustness of the results is compared by box plots. Figure 12 shows the box plots of the relative errors of the mean of the results obtained by the three methods with 100 samples. Figure 13 shows the box plots of the relative errors of the mean of the results obtained by the AFBS with 30, 50 and 100 samples, respectively. Figure 14 shows the box plots of the relative errors of the standard deviation of the results obtained by the three methods with 100 samples. Figure 15 shows the box plots of the relative errors of the standard deviation of the results obtained by AFBS with 30, 50 and 100 samples, respectively. The results indicate that at the same number of samples, the interquartile range of the relative error in predicting the mean of AFBS is smaller than that of OMP and OLS, and the interquartile range, mean, and median of the relative error in predicting the standard deviation of AFBS are much smaller than those of OMP and OLS. The interquartile range of AFBS decreases with samples increasing. The outliers of the mean and standard deviation predicted by the OLS and OMP methods are significantly larger and more compared to the AFBS method. Therefore, the sparse PC reconstruction method based on AFBS method is more reliable and effective than the OMP and OLS methods and can meet complex engineering problems requirements.

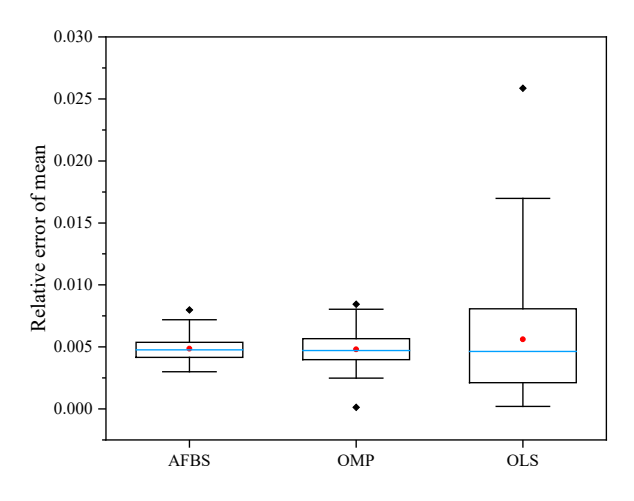


Figure 12 – Relative error of the mean predicted by the AFBS, OMP, and OLS (100 samples, calculated 100 times).

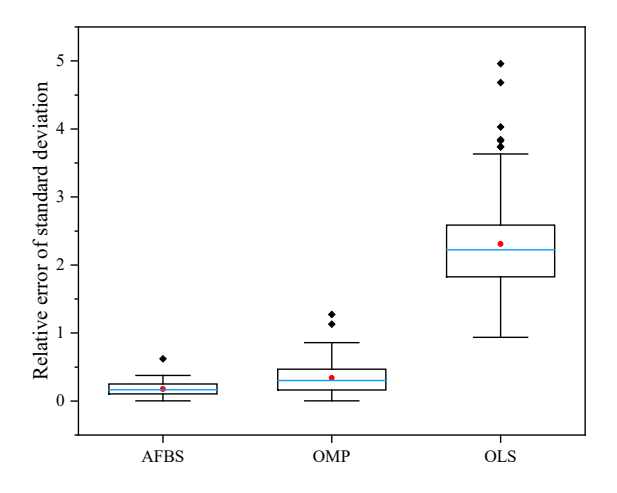


Figure 14 – Relative error of the standard deviation of the AFBS, OMP, and OLS predictions (100 samples, calculated 100 times).

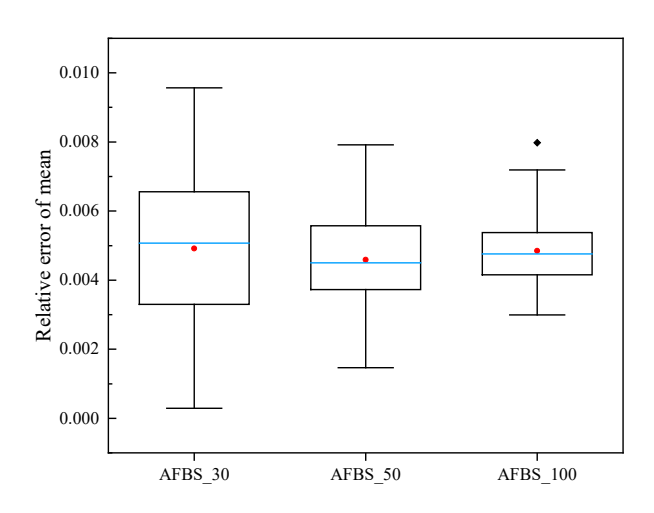


Figure 13 – Relative error of the mean predicted by the AFBS with 30, 50 and 100 samples (calculated 100 times).

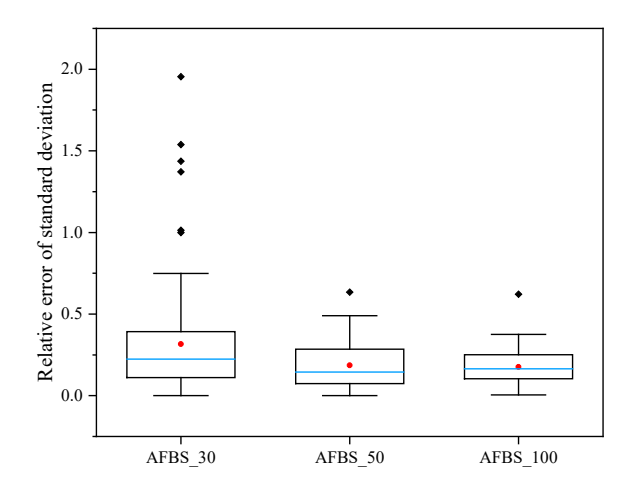


Figure 15 – Relative error of the standard deviation predicted by the AFBS with 30, 50 and 100 samples (calculated 100 times).

4. Aerodynamic/sonic boom robust design optimization framework

In this chapter, the JAXA Wing Body (JWB), a sonic boom configuration from JAXA, Japan, is used to perform a robust design optimization considering both aerodynamic and sonic boom. The model and design parameters are provided from the Second Sonic Boom Prediction Workshop (SBPW2). The CFD simulations and sonic boom calculations are performed using half-models with the parameter settings shown in Table 1.

Table 1 CFD simulation parameter settings

Mach	Alpha	Body	Reference	Altitude	Temperature	Reynolds	
number	Дірпа	length	area	Ailliude		Number	
1.6	2.3067°	38.7 m	$32.8m^2$	15760 m	216.65 <i>K</i>	5.7E6	

The traditional aerodynamic design optimization mainly considers lift, drag, moment coefficient. The sonic boom optimization considers the sonic boom ground sensory noise level (PLdB), which was firstly proposed by Stevens [31], and then modified by Shepherd [32] to enable it to analyze low-frequency noise. The quantification of noise intensity at different frequencies is very consistent with the real response of the human ear, so it has been widely used by sonic boom researchers.

Robust design optimization requires consideration of the effects of uncertainty sources, and in this chapter two uncertain parameters are considered: Mach number $Ma \sim N(1.6, 0.01)$ and angle of attack $\alpha \sim N(2.3067, 0.01)$. The aerodynamic optimization parameters are mean and standard deviation of the lift coefficient, mean and standard deviation of the drag coefficient, standard deviation of the pitching moment coefficient. And the optimization parameter for the acoustic boom is: mean and standard deviation of the perceived sound pressure level PLdB. The constraints are the optimized thickness of the three positions of the wing is not thinner and the pitching moment coefficient of the whole aircraft is not worse after optimization. The mathematical representation is shown in(12).

Condition: Re =
$$5.7 \times 10^6$$

$$Ma \in N(1.6, 0.01^2)$$

$$\alpha \in N(2.3067, 0.01^2)$$
Find: $\mathbf{X} \in \mathbb{R}^n$

$$\begin{cases} u_{c_l}(Ma, \alpha) \\ \sigma_{C_l}(Ma, \alpha) \\ u_{c_d}(Ma, \alpha) \end{cases}$$
Minimize:
$$\begin{cases} \sigma_{C_d}(Ma, \alpha) \\ \sigma_{C_my}(Ma, \alpha) \\ \sigma_{C_my}(Ma, \alpha) \\ \sigma_{PLdB}(Ma, \alpha) \end{cases}$$
Subject to: $|C_m| \leq |C_{m0}|$

$$Thick \geq T_0$$

$$(12)$$

The optimization process is shown in Figure 16.

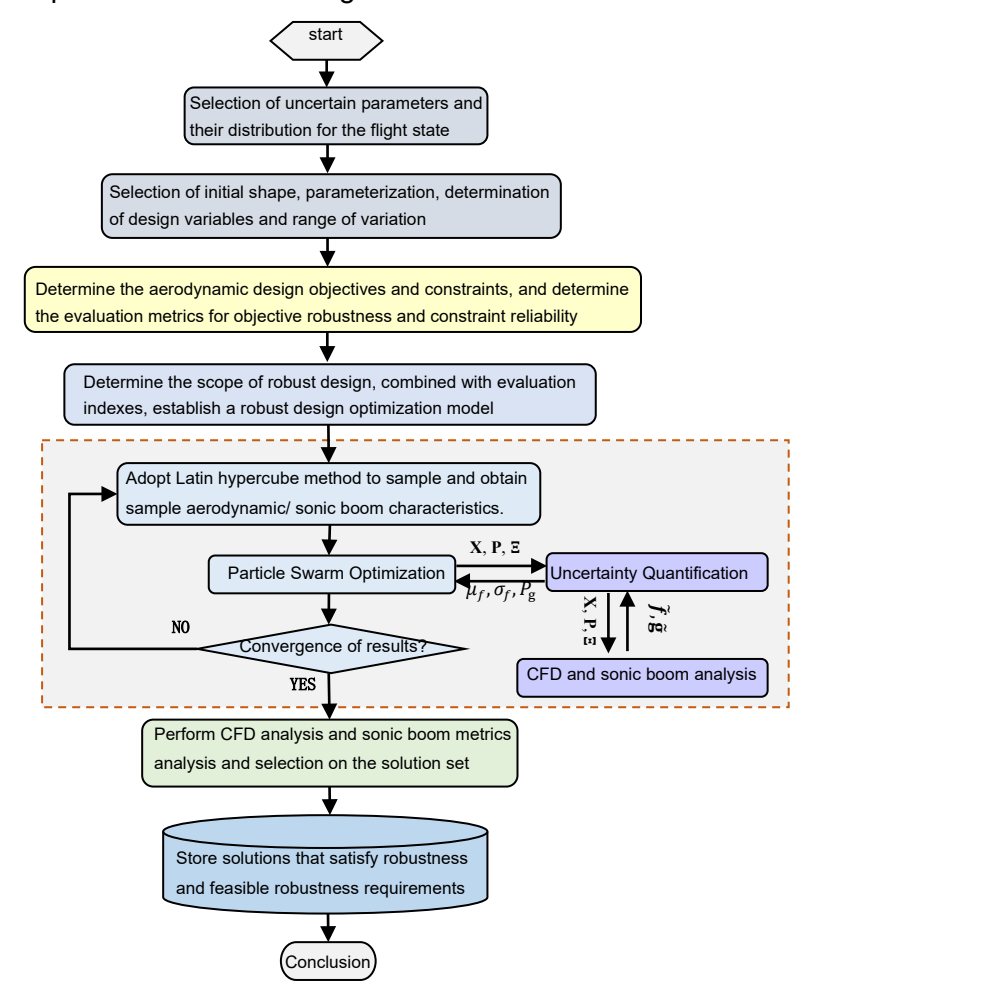


Figure 16 – Aerodynamic/sonic boom robust design optimization flowchart

Using the FFD method based on multiple control frames, the deformation control of the shape is realized by using multiple non-rectangular control frames. A total of 30 design variables are set, of which the control box is shown in Figure 17 and is divided into fuselage control points and wing control points. There are 12 fuselage control points, 6 on each of the upper and lower surfaces. There are 18 wing control points, which are divided into three segments from the inner wing to the outer wing, and 3 control points on each of the upper and lower surfaces. The displacement direction of the control points is set to z-direction at the fuselage control points and x-direction at the wing control points.

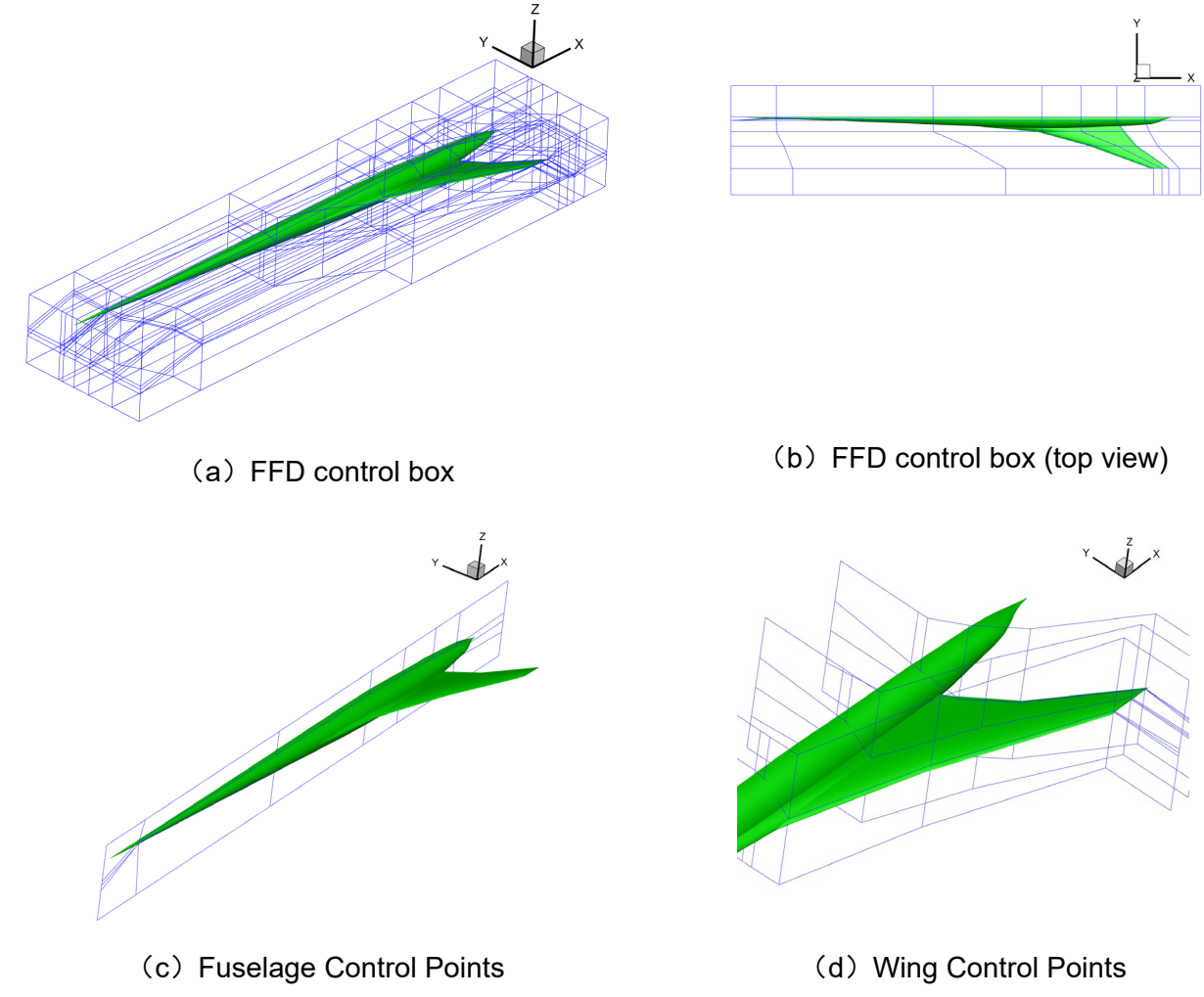


Figure 17 – FFD Control Box Setting

The optimization process is carried out by constructing a Kriging agent model. New shapes are obtained by searching using a particle swarm optimization algorithm. The resulting new shape is generated using a fast mesh deformation method based on multi-block structured meshes constructed using bulk spline interpolation and infinite interpolation techniques. The solver was CFL3D using the Spalart-Allmaras turbulence model [33].

5. Result of aerodynamic/sonic boom robust optimization

5.1 Comparison of shape before and after optimization

Comparison of the deformation at the fuselage and wing between the new shape and the original shape after optimization is shown in Figure 18 and Figure 19. The new shape has a certain upward shift at the nose, which disappears after a certain distance. The lower surface of the fuselage begins to move down a bit, resulting in a "taper" at the front of the nose. The aft fuselage is also more pronounced than the original shape. The main changes to the wings are: a small rearward shift of the leading edge of the inner wing, a small forward shift of the trailing edge, a significant forward shift of the trailing edge of the center wing, and a small forward shift of the leading edge of the outer wing.

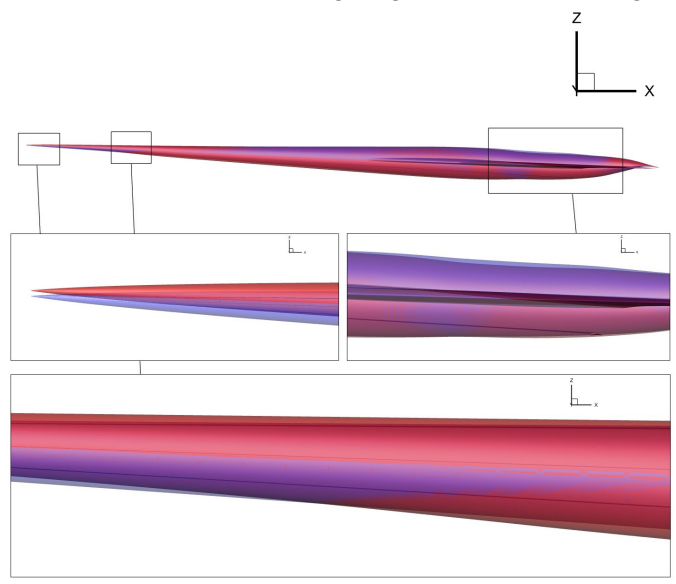


Figure 18 – Comparison of body before and after optimization (original shape in blue, optimized shape in red)

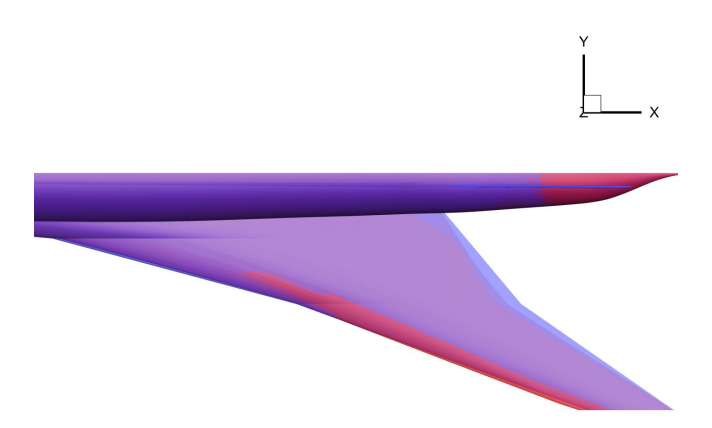


Figure 19 – Comparison of the wing before and after optimization (original shape in blue, optimized shape in red)

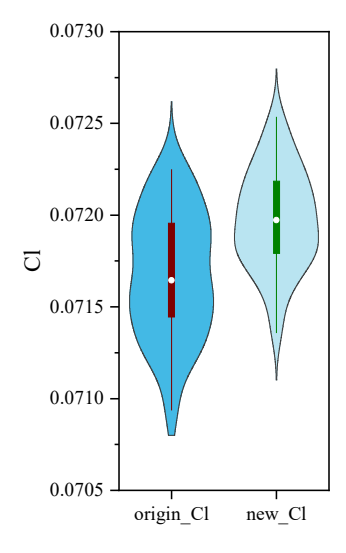
5.2 Comparison of aerodynamic and sonic boom performance before and after optimization

This optimization is a robust design optimization, so each metric is the mean and standard deviation of the mean and standard deviation calculated from 50 samples taken from the shape before and after the optimization with Mach number and angle of attack as sources of uncertainty. The changes in the aerodynamic/sonic boom performance metrics before and after the optimization are given in Table 2, and Figure 20 is a violin plot with box showing the distribution of these sample points under the influence of uncertainty sources.

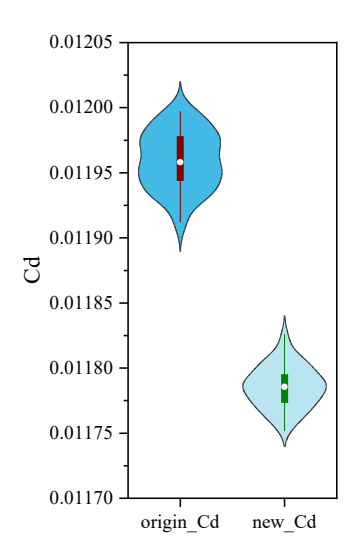
The results show that the mean values of lift, drag, moment and PLdB have a better mean value after optimization and the standard deviation of each has decreased, i.e. better robustness. The violin plot also shows that the length of the box is smaller, i.e., the distribution of data points becomes more concentrated.

Table 2 Comparison of aerodynamic sonic boom indexes before and after optimization

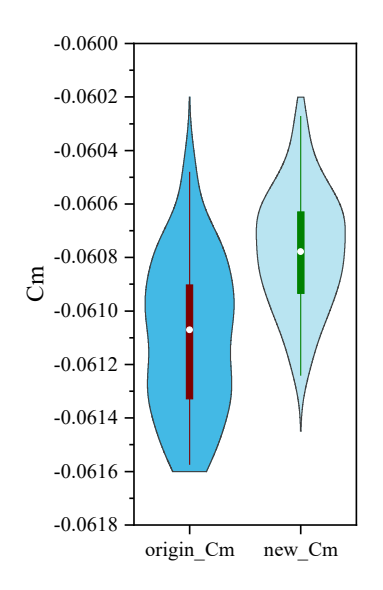
	μ_{C_l}	$\sigma_{\scriptscriptstyle C_l}$	μ_{C_d}	$oldsymbol{\sigma}_{C_d}$	μ_{C_m}	$\sigma_{\scriptscriptstyle C_m}$	$\mu_{{\scriptscriptstyle PLdB}}$	$\sigma_{\scriptscriptstyle PLdB}$
Origin	0.07167	3.38E-04	0.01196	2.18E-05	-0.06109	2.81E-04	69.55102	0.50278
New	0.07197	2.72E-04	0.01179	1.66E-05	-0.06077	2.21E-04	67.54449	0.47884
Elevation	0.42%	19.41%	1.46%	23.95%	0.53%	21.25%	2.88%	4.76%

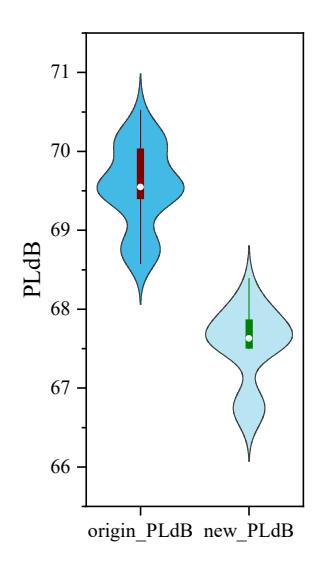


(a) C_l distribution of profile sample points before and after optimization



(b) C_d distribution of profile sample points before and after optimization





(c) $C_{\scriptscriptstyle m}$ distribution of profile sample points before and after optimization

(d) *PLdB* distribution of profile sample points before and after optimization

Figure 20 – Distribution of sample points before and after optimization

6. Conclusion

6.1 Uncertainty quantification of sonic boom

With the increasing performance requirements of aircraft and the development of advanced computational power, it is important to consider the effects of various possible parameters of uncertainty in the design process and design an aircraft with robust performance. However, traditional aerodynamic UQ methods that consider multi-parameter uncertainties, such as MCS and full PCE, cannot avoid the high computational cost and have poor adaptability. These make them difficult to meet the requirements of complex sonic boom UQ. To address this difficulty, this paper uses an efficient sparse polynomial chaos reconstruction method based on adaptive forward-backward selection (AFBS), combined with the augmented Burgers equation, to quantify the uncertainty of far-field sonic boom prediction. The AFBS method effectively enhances the sparsity of the PC reconstruction and improves the reliability of the fitting process. The augmented Burgers equation accurately simulates the far-field propagation of sonic boom. Combining the two methods increases the accuracy of sonic boom prediction. The paper carries out sonic boom UQ considering six uncertain parameters: Mach number, altitude, temperature, humidity, wind direction, and wind velocity, and compares the results with the OMP method and the OLS method. The results indicate that the AFBS method is more accurate in estimating the ground sonic boom signature compared to the OMP and OLS methods with the same sample size. In particular, the results obtained by AFBS are less affected by sample variation although the sample size is small. Therefore, the efficient sparse PC reconstruction method based on AFBS is less computational cost and accurate. It can be used for complex sonic boom UQ under multi-parameter uncertainties and robust multidisciplinary optimal design of aircraft.

6.2 Aerodynamic / sonic boom robust optimization

Through the aerodynamic sonic boom robust design optimization of JWB shape and the corresponding results of analysis. The resulting new shape in the set indicators of better performance and more robust to the influence of external uncertainty sources. The optimized new shape has a thinner nose, the rear fuselage convergence, the wing chord of the smaller characteristics, which meet the common characteristics of the supersonic aircraft. The conclusions of this work for the subsequent sonic boom optimization of shape deformation settings to provide guidance.

This optimization also found some problems, such as the proxy model predictions and the actual results of the mean value is more similar, but the standard deviation prediction is more inaccurate, which will lead to robust optimization results may not be to meet the needs. Sonic boom evaluation index only consider PLdB will lose a lot of information. Need to further measure the sonic boom "N-shaped wave" of a variety of indicators: maximum overpressure, rise time, duration, pulse value, etc. into the measurement criteria, so that the results obtained to better meet the characteristics of the low sonic boom waveform. However, if the subsequent need to increase the optimization index, due to the consideration of the optimization index increases, the optimization algorithm will gradually become inefficient, so the subsequent need to choose a more efficient optimization algorithm.

7. Contact Author Email Address

Huan Zhao: huanzhao@nwpu.edu.cn

8. Copyright Statement

The authors confirm that they, and/or their company or organization, hold copyright on all of the original material included in this paper. The authors also confirm that they have obtained permission, from the copyright holder of any third party material included in this paper, to publish it as part of their paper. The authors confirm that they give permission, or have obtained permission from the copyright holder of this paper, for the publication and distribution of this paper as part of the ICAS proceedings or as individual off-prints from the proceedings.

9. Acknowledgement

This research was sponsored by the National Natural Science Foundation of China (NSFC) under Grant No. 12102489.

References

- [1] Shimoyama K and Inoue A. Uncertainty Quantification by the Nonintrusive Polynomial Chaos Expansion with an Adjustment Strategy. *AIAA Journal*, Vol. 54, No. 10, pp. 3107–3116, 2016.
- [2] West T K, Reuter B W, Walker E L, Kleb B, and Park M A. Uncertainty Quantification and Certification Prediction of Low-Boom Supersonic Aircraft Configurations. *Journal of Aircraft*, Vol. 54, No. 1, pp. 40–53, 2017.
- [3] Walker E, Pinier J T, West T and Bretl K. Sonic Boom Pressure Signature Uncertainty Calculation and Propagation to Ground Noise (Invited). *53rd AIAA Aerospace Sciences Meeting, Kissimmee*, Florida, 2015.
- [4] Jeong S, Ono D, Shimoyama K and Hashimoto A. Sonic Boom Analysis under Conditions of Atmospheric Uncertainty Using Polynomial Chaos. *TRANSACTIONS OF THE JAPAN SOCIETY FOR AERONAUTICAL AND SPACE SCIENCES*, Vol. 56, No. 3, pp. 129–136, 2013.
- [5] Colonno M and Alonso J. Sonic Boom Minimization Revisited: The Robustness of Optimal Low-Boom Designs. *13th AIAA/ISSMO Multidisciplinary Analysis Optimization Conference*, Fort Worth, Texas, 2010.
- [6] Emre Tekaslan H, Yildiz S, Demiroglu Y and Nikbay M. Implementation of Multidisciplinary and Multifidelity Uncertainty Quantification Methods for Sonic Boom Prediction. *Journal of Aircraft*, Vol. 60, No. 2, pp. 410–422, 2023.
- [7] Makino Y and Kroo I. Robust Objective Functions for Sonic-Boom Minimization. *Journal of Aircraft*, Vol. 43, No. 5, pp. 1301–1306, 2006.
- [8] Schaefer J A, Lazzara D S and LeDoux S T. Robust Design of Sonic Boom Performance Using Spatially Accurate Polynomial Chaos. *AIAA SCITECH 2023 Forum, National Harbor*, MD & Online, 2023.
- [9] Rallabhandi S K, West T K and Nielsen E J. Uncertainty Analysis and Robust Design of Low-Boom Concepts Using Atmospheric Adjoints. *Journal of Aircraft*, Vol. 54, No. 3, pp. 902–917, 2017.
- [10] Zang T A, Hemsch M J, Hilburger M W, Kenny S P, Luckring J M, Maghami P, Padula S L and Stroud W J. Needs and Opportunities for Uncertainty- Based Multidisciplinary Design Methods for Aerospace Vehicles. 2002.
- [11] Zhao K, Gao Z and Huang J. Robust Design of Natural Laminar Flow Supercritical Airfoil by Multi-Objective Evolution Method. *Applied Mathematics and Mechanics*, Vol. 35, No. 2, pp. 191–202, 2014.
- [12] Zhao H and Gao Z. Uncertainty-Based Design Optimization of NLF Airfoil Based on Polynomial Chaos Expansion. *The Proceedings of the 2018 Asia-Pacific International Symposium on Aerospace Technology (APISAT 2018)*, edited by X. Zhang, Vol. 459, Springer Singapore, Singapore, pp. 1576–1592, 2019.
- [13] Jiangtao H, Zhenghong G, Ke Z and Junqiang B. Robust Design of Supercritical Wing Aerodynamic Optimization Considering Fuselage Interfering. *Chinese Journal of Aeronautics*, Vol. 23, No. 5, pp. 523–528, 2010.
- [14] Zhao H, Gao Z, Xu F, Zhang Y and Huang J. An Efficient Adaptive Forward–Backward Selection Method for Sparse Polynomial Chaos Expansion. *Computer Methods in Applied Mechanics and Engineering*, Vol. 355, pp. 456–491, 2019.
- [15] Keane A J. Cokriging for Robust Design Optimization. AIAA Journal. Vol. 50, No. 11, pp 2285-2626, 2012.

- [16] Hosder S, Walters R and Perez R. A Non-Intrusive Polynomial Chaos Method For Uncertainty Propagation in CFD Simulations. 44th AIAA Aerospace Sciences Meeting and Exhibit, Reno, Nevada, 2006.
- [17] Shah H, Hosder S and Winter T. Quantification of Margins and Mixed Uncertainties Using Evidence Theory and Stochastic Expansions. *Reliability Engineering & System Safety*, Vol. 138, pp. 59–72, 2015.
- [18] Padron A S, Alonso J J and Eldred M S. Multi-Fidelity Methods in Aerodynamic Robust Optimization. *18th AIAA Non-Deterministic Approaches Conference*, San Diego, California, USA, 2016.
- [19] Dodson M and Parks G T. Robust Aerodynamic Design Optimization Using Polynomial Chaos. *Journal of Aircraft*, Vol. 46, No. 2, pp. 635–646, 2009.
- [20] Xiu D and Karniadakis G E. The Wiener--Askey Polynomial Chaos for Stochastic Differential Equations. *SIAM Journal on Scientific Computing*, Vol. 24, No. 2, pp. 619–644, 2002.
- [21] Donoho D L. Compressed Sensing. IEEE Transactions on Information Theory, Vol. 52, No. 4, pp. 1289–1306, 2006.
- [22] Rauhut H and Ward R. Sparse Legendre Expansions via & 1 -Minimization. *Journal of Approximation Theory*, Vol. 164, No. 5, pp. 517–533, 2012.
- [23] Efron B, Hastie T, Johnstone I and Tibshirani R. LEAST ANGLE REGRESSION. *The Annals of Statistics*, Vol. 32, No. 2, 407–499, 2004.
- [24] Tropp J A and Gilbert A C. Signal Recovery From Random Measurements Via Orthogonal Matching Pursuit. *IEEE Transactions on Information Theory*, Vol. 53, No. 12, pp. 4655–4666, 2007.
- [25] Peng J, Hampton J and Doostan A. A Weighted -Minimization Approach for Sparse Polynomial Chaos Expansions. *Journal of Computational Physics*, Vol. 267, pp. 92–111, 2014.
- [26] Guo L, Narayan A and Zhou T. A Gradient Enhanced &1-Minimization for Sparse Approximation of Polynomial Chaos Expansions, *Journal of Computational Physics*, Vol. 367, pp. 49–64, 2018.
- [27] Salehi S, Raisee M, Cervantes M J and Nourbakhsh A. An Efficient Multifidelity ℓ 1 -Minimization Method for Sparse Polynomial Chaos. *Computer Methods in Applied Mechanics and Engineering*, Vol. 334, pp. 183–207, 2018.
- [28] Blatman G and Sudret B. Adaptive Sparse Polynomial Chaos Expansion Based on Least Angle Regression. *Journal of Computational Physics*, Vol. 230, No. 6, pp. 2345–2367, 2011.
- [29] Zhang Y, Huang J and Gao Z. Far Field Simulation and Applications of Sonic Boom Based on Augmented Burgers Equation. *Hangkong Xuebao/Acta Aeronautica et Astronautica Sinica*, Vol. 39, 2018.
- [30] BW Y. Formulization of Standard Atmospheric Parameters. *Chinese Society of Astronautics Journal*, Vol. 1, 1983
- [31] Stevens S S. Perceived Level of Noise by Mark VII and Decibels (E). The Journal of the Acoustical Society of America, Vol. 51, No. 2B, pp. 575–601, 1972.
- [32] Shepherd P and Sullivan M. A Loudness Calculation Procedure Applied to Shaped Sonic Booms.
- [33] Spalart P and Allmaras S. A One-Equation Turbulence Model for Aerodynamic Flows. *30th Aerospace Sciences Meeting and Exhibit*, Reno, NV, U.S.A., 1992.